

The evolution of low-metallicity asymptotic giant branch stars and the formation of carbon-enhanced metal-poor stars

Herbert H. B. Lau^{1,2,3*}, Richard J. Stancliffe^{2,3} and Christopher A. Tout²

¹*Kavli Institute for Astronomy & Astrophysics, Peking University, China*

²*Institute of Astronomy, The Observatories, Madingley Road, Cambridge CB3 0HA*

³*Centre for Stellar and Planetary Astrophysics, School of Mathematics, Building 28, Monash University, Clayton VIC 3800, Australia*

Accepted 2009 March 12. Received 2009 March 12; in original form 2009 February 16

ABSTRACT

We investigate the behaviour of asymptotic giant branch (AGB) stars between metallicities $Z = 10^{-4}$ and $Z = 10^{-8}$. We determine which stars undergo an episode of flash-driven mixing, where protons are ingested into the intershell convection zone, as they enter the thermally pulsing AGB phase and which undergo third dredge-up. We find that flash-driven mixing does not occur above a metallicity of $Z = 10^{-5}$ for any mass of star and that stars above $2 M_{\odot}$ do not experience this phenomenon at any metallicity. We find carbon ingestion (CI), the mixing of carbon into the tail of hydrogen burning region, occurs in the mass range $2 M_{\odot}$ to around $4 M_{\odot}$. We suggest that CI may be a weak version of the flash-driven mechanism. We also investigate the effects of convective overshooting on the behaviour of these objects. Our models struggle to explain the frequency of CEMP stars that have both significant carbon and nitrogen enhancement. Carbon can be enhanced through flash-driven mixing, CI or just third dredge up. Nitrogen can be enhanced through hot bottom burning and the occurrence of hot dredge-up also converts carbon into nitrogen. The C/N ratio may be a good indicator of the mass of the primary AGB stars.

Key words: stars: evolution, stars: AGB and post-AGB, stars: carbon

1 INTRODUCTION

In recent years, there has been considerable interest in the observation of metal-poor stars and particularly those of a carbon-rich nature. A surprising fraction of stars with metallicities below $[\text{Fe}/\text{H}]$ of around -2.5 are found to be rich in carbon. This fraction, while uncertain, may be as high as around 20 per cent (Lucatello et al. 2006). Many of these stars display evidence of s -process enrichments. It has been proposed that they may be formed by mass transfer in binary systems. Such a system would consist of two stars in a wide orbit. The primary star evolves to the asymptotic giant branch (AGB) where it becomes enriched in carbon (and also s -process elements). Strong mass loss strips the envelope from this star which becomes a white dwarf and fades from view. The star is losing mass so some of this is accreted by the companion which becomes carbon-rich. It is this companion that we see today. Credence is lent to this argument by the observation that, of the carbon and s -process rich stars, around 70 per cent are found to be members of bi-

nary systems (Lucatello et al. 2005). This is consistent with the whole population being binaries.

This scenario may be complicated somewhat. It has commonly been assumed that, when the material is accreted on to the companion, it remains on the surface of the recipient star. However, Stancliffe et al. (2007) showed that thermohaline mixing can lead to this accreted material being extensively mixed with the pristine matter of the companion and this can have important consequences for the abundances that would be observed in such an object. The extent of this mixing depends on the composition and mass of accreted material, as well as the evolutionary state of the accreting star (see Stancliffe & Glebbeek 2008). However, we may still hope to observe the signatures of low-metallicity AGB stars in the compositions of the CEMP stars that are still visible today. To do this demands that we know what the expected nucleosynthetic signatures of the parent AGB stars are.

The asymptotic giant branch (AGB) is a late phase of stellar evolution for stars with masses from 1 to around $8 M_{\odot}$. It follows the end of the core helium burning phase. As the core of the star runs out of helium it begins to ascend

* hlau@kiaa.pku.edu.cn

the AGB. The star first expands and cools and the convective envelope deepens. The envelope can reach down as far as the hydrogen burning shell, pulling material to the surface and altering the surface composition of the star. This is the second dredge-up

Helium and hydrogen are both burning in thin shells. The helium burning shell slowly moves outwards in mass and the region between the two shells narrows. When they get very close (separated by a few hundredths of a solar mass) the star enters the thermally pulsing asymptotic giant branch (TP-AGB) phase. Thermal pulses are the rapid increase in the helium-burning luminosity to over $10^8 L_{\odot}$, for a brief period of time, usually around 10yr. The thermal pulses are a consequence of the thinness of the helium burning shell and high temperature sensitivity of the triple- α reaction. The theory is described, for AGB stars, by Schwarzschild & Härm (1965). When energy is dumped in the thin shell, the temperature can rise when the shell expands. There is no thermostatic control until the shell is no longer thin. Also, for the pulse to occur, the increased radiative losses owing to the increase of shell temperature must not carry energy away faster than it is being generated. This is usually fulfilled because helium burning is highly sensitive to temperature. Yoon, Langer & van der Sluys (2004) have investigated the stability of shell sources and find that the helium burning shell tends to be more stable at high temperature because the triple- α reaction is less temperature sensitive.

During the thermal pulses, the sudden increase in energy release, caused by enhanced helium burning, leads to convection between the two burning shells and mixes the ashes of helium burning outwards from the helium burning shell. The star expands and the hydrogen burning shell cools and may be extinguished. Eventually thermostatic control is restored in the He-shell, the helium luminosity starts to drop and the intershell convection region shuts down. The convective envelope deepens during this power down phase, which lasts for about 100 yr. The envelope could penetrate into regions where the intershell convection zone had been active (Iben 1975). This means that the carbon that has been produced during helium burning is ingested by the envelope. This is called third dredge-up (TDUP). The surface is then enriched in carbon (and *s*-process elements¹). The base of the convective envelope can be hot enough for some CNO cycle reactions to occur, particularly for stars more massive than $4 M_{\odot}$. This is called hot bottom burning (HBB). Helium burning returns to a quiescent state and the hydrogen shell reignites. Helium accumulates again during this inter-pulse period which can last over 1,000 yr. The cycle then repeats and may do so many times before stellar winds can strip away the envelope.

Low-metallicity AGB stars are known to evolve differently to their higher metallicity counterparts. In the case of the low-mass objects it is possible for the helium-burning driven intershell convection zone to penetrate into the hydrogen-rich envelope (Fujimoto et al. 2000). This does

not happen at higher metallicity because the hydrogen burning shell presents an effective entropy barrier which inhibits the advance of the intershell convection zone. As the metal content of the star is reduced, hydrogen burning via the CNO cycle is weaker and presents less of a barrier. Below some critical metallicity, the intershell zone manages to penetrate into H-rich regions. This leads to hydrogen being dragged down to regions of high temperature, with vigorous H-burning occurring as a result. The convective region can then split in to two separate zones, one driven by H-burning, the other by He-burning. This phenomenon is referred to as flash driven mixing (FDM, Suda et al. 2004). It has been reported by several authors, including Fujimoto et al. (2000) and Campbell & Lattanzio (2008).²

Metal-free evolution for low- and intermediate-mass stars has been explored by Chieffi et al. (2001) and Siess et al. (2002). Chieffi et al. (2001) find that during thermal pulses of AGB stars at or below $5 M_{\odot}$, a convective shell forms at the H-He interface and the subsequent expansion of this convective shell in to the underlying layers previously occupied by the pulse dredges up some carbon and initiates an H flash. In the paper, this phenomenon is referred as carbon ingestion (CI). Siess et al. (2002) also find this unusual convective shell and that there is a mixing episode for stars at or below $6 M_{\odot}$. They also refer to it as CI.

In addition, Herwig (2004) reported that, at a metallicity of $Z = 10^{-4}$, the nature of third dredge-up changes. With the inclusion of convective overshooting, he found that hydrogen would actually burn *during* TDUP and that the propagation of a H-burning flame could erode the entire intershell and even dredge up some material from the CO core. This behaviour has been dubbed hot dredge-up.

Our purpose in this work is to delineate the boundaries between these regimes of behaviour. This will enable us to place limits on which stars are able to produce which nucleosynthetic signatures. Based on our models, we can hope to explain the variation of carbon and nitrogen enrichment of CEMP stars in terms of the different enrichment processes of extremely metal-poor AGB stars of different masses. Therefore, the observed frequencies of different types of CEMP stars may tell us the relative numbers of low- and high-mass AGB stars in extremely metal-poor environments. This can help deduce the form of the initial mass function at low metallicity (see e.g. Lucatello et al. 2005).

2 STELLAR EVOLUTION CODE

We use the stellar evolution code STARS which is a variant of that originally developed by Eggleton (1971) and updated by many authors (e.g. Pols et al. 1995). The version used here includes the AGB-specific modifications of Stancliffe, Tout & Pols (2004), together with the updated opacity tables of Eldridge & Tout (2004) which account for the enhancement to the opacity from enhancements in carbon and oxygen abundance. The code has been extensively

¹ The *s*-process is the capture of neutrons by nuclei in conditions of sufficiently low neutron density that any unstable products have time to decay before another neutron is captured. The neutron source in AGB stars is not yet properly understood.

² The community is yet to accept a standard nomenclature for these events. They have also been called ‘proton ingestion episodes’ (Cristallo et al. 2007) and ‘dual shell flashes’ (Campbell & Lattanzio 2008).

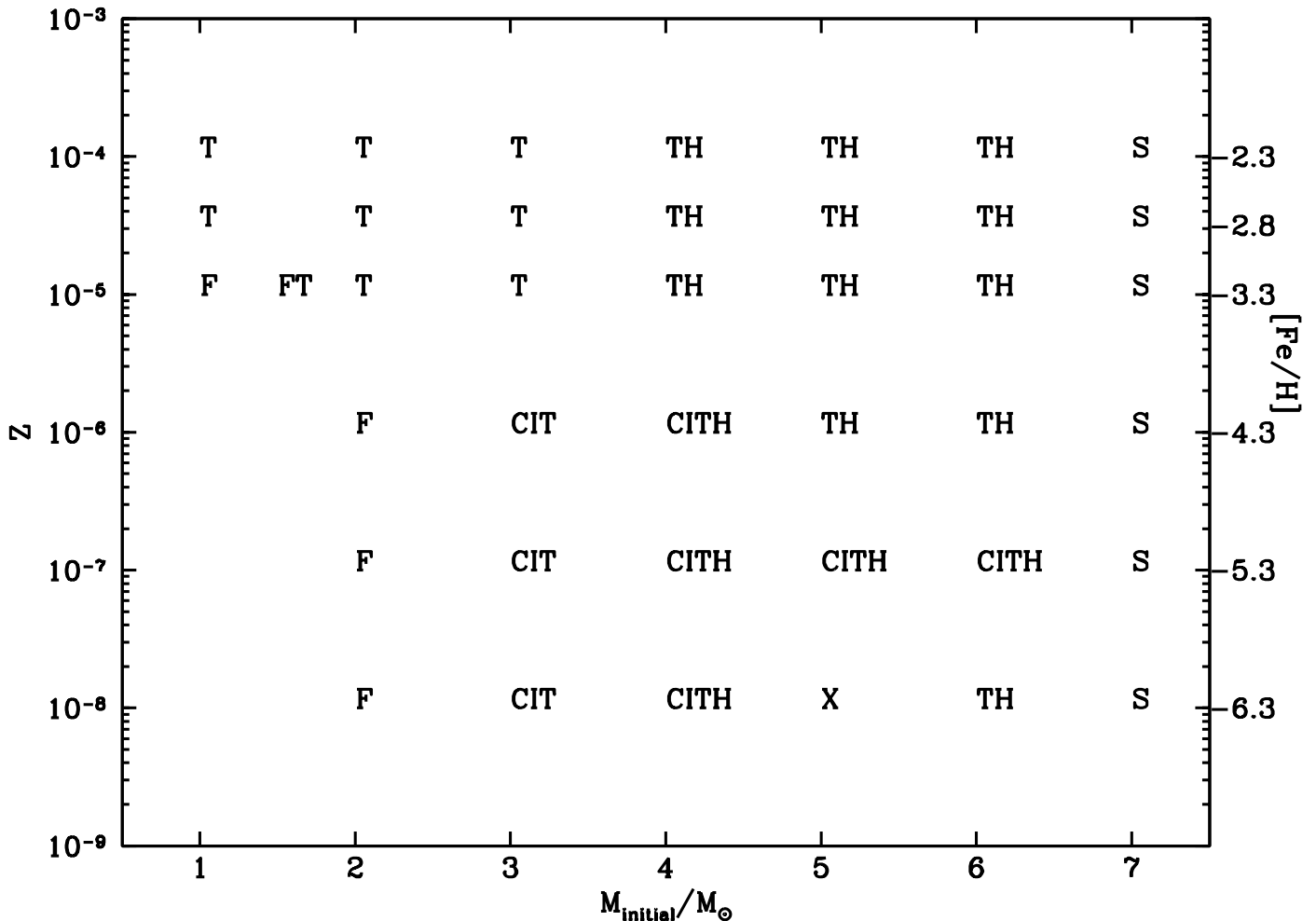


Figure 1. AGB behaviour of the models as a function of mass and metallicity without overshooting. The symbols are T – the model undergoes third dredge-up, H – the model undergoes hot third dredge-up, F – the model undergoes flash-driven mixing, CI – the model undergoes a carbon injection, X – no TDUP occurs, S – the model undergoes carbon ignition before the AGB and presumably becomes an S-AGB star.

used to compute TP-AGB evolution in recent years (see e.g. Stancliffe et al. 2005; Lau et al. 2007)

We do not apply mass loss at any stage of evolution. Mass-loss rates for AGB stars are very uncertain and it is expected that mass loss scales with metallicity. In any case, the behaviour we are interested in happens in the first few pulses before any mass loss would be significant. We use $\alpha = 2.0$ for the mixing length parameter in the Böhm-Vitense (1958) prescription. This value is chosen based on calibration to a solar model. We also chose solar-scaled initial abundances (Anders & Grevesse 1989) rather than attempting to follow the chemical evolution of the Galaxy.

We have made models of metallicity $Z = 10^{-4}, 3 \times 10^{-5}, 10^{-5}, 10^{-6}, 10^{-7}, 10^{-8}$ and 0. We have not modelled the lowest-mass stars at the lowest metallicities because these stars undergo a helium flash. The STARS code is currently unsuitable for modelling this phase in a star’s evolution. While it is possible to generate a post-He flash model (see Stancliffe & Jeffery 2007, for details), the method assumes that the envelope composition is unaffected by the

helium flash and this cannot be guaranteed below a metallicity of $[\text{Fe}/\text{H}] < -4.5$ (Fujimoto et al. 1990).

The models are evolved from the pre-main sequence to the TP-AGB with 999 mesh points. At the beginning of the TP-AGB, the AGB-specific mesh spacing function of Stancliffe et al. (2004) is switched on. It is also at this point that the AGB mixing prescription by the same authors is applied. In the initial runs, no convective overshooting was applied at any phase in the star’s evolution.

3 RESULTS

We can roughly divide the evolutionary behaviour of these extremely metal-poor stars into five different regimes, (i) stars with a flash-driven mixing episode, (ii) stars with CI, (iii) stars with no third dredge-up, (iv) stars that experience third dredge-up which can be subdivided depending on whether hot dredge-up or hot bottom burning or both are present and (v) stars which undergo carbon ignition before

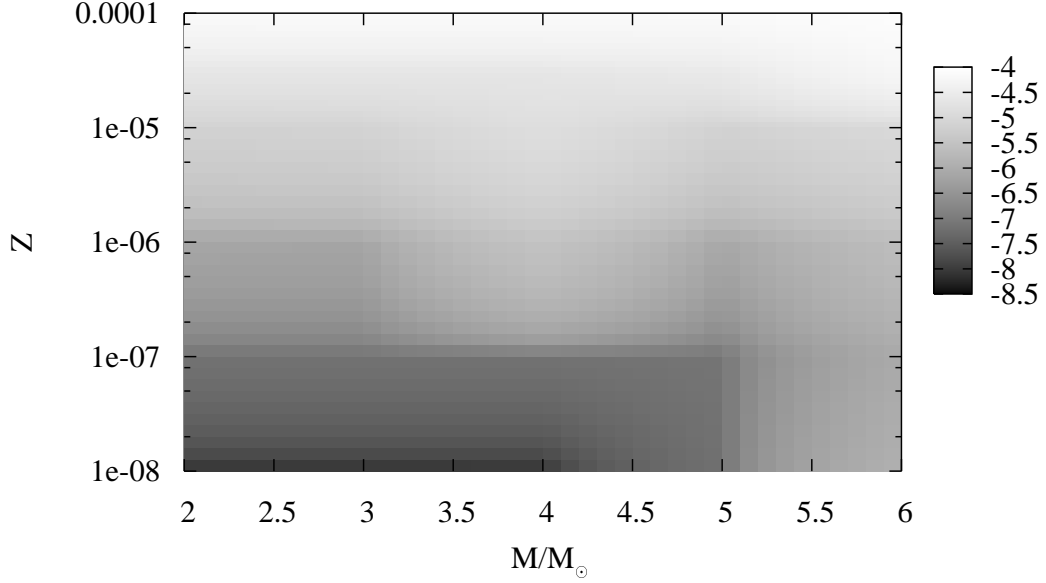


Figure 2. The abundance of CNO elements by mass at the beginning of the TP-AGB. The action of second dredge-up substantially raises the abundance in the case of the intermediate-mass stars.

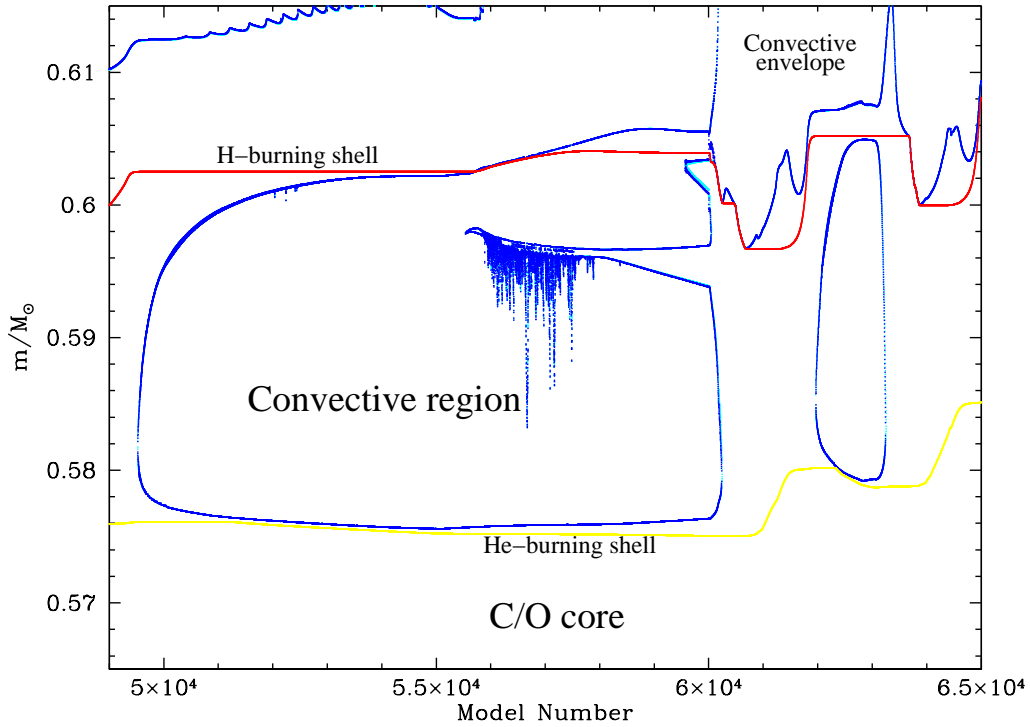


Figure 3. Evolution of $1.5 M_{\odot}$, $Z = 10^{-5}$ model during He-FDM. We can see the convective region reaches the H-burning shell at model number around 56000. The messy appearance is due to numerical problems to resolve the mixing episode. The 2nd pulse, at about model 62,000 is simply a normal thermal pulse.

the AGB. These regimes of behaviour are shown in Fig. 1 in mass and metallicity space.

Stars with an initial mass of $7 M_{\odot}$ or above become super-AGB (SAGB) when carbon is ignited non-degenerately before any thermal pulses (Gil-Pons et al. 2005). We do not follow the evolution of such SAGB stars, owing to the considerable complexity involved in their computation (Siess 2006). It is worth noting that a different mixing-length parameter α could change the critical mass at which a star becomes an SAGB star. For example, a $7 M_{\odot}$ model of $Z = 10^{-8}$ evolved with $\alpha = 1.925$ does not evolve into a SAGB star. This is a perfect example to show that the mixing length parameter is crucial to determine the evolution of extremely-metal poor stars (and in fact, any star). In this work all models are computed with $\alpha = 2.0$ and we shall examine the effect of varying it in the future.

Stars with $Z = 10^{-4}$ (corresponding to $[\text{Fe}/\text{H}] \approx -2.3$) behave similarly to their higher metallicity cousins, with the occurrence of third dredge up and hot bottom burning. This suggests that AGB stars with $Z = 10^{-4}$ have enough CNO elements in the hydrogen burning shell that their evolution is not affected by the low metallicity. When the metallicity is decreased to $Z = 10^{-5} - 10^{-6}$, the high mass AGB stars still behave as they do at higher metallicity, in that they experience only thermal pulses, third dredge-up and hot bottom burning. This is because second dredge-up is more efficient in higher mass stars and leads to an increased CNO abundance in the envelope and (more importantly) the hydrogen burning shell (see Fig. 2). Therefore, the amount of metals, particularly the CNO elements in the hydrogen burning shell is one of the important factors in determining the evolutionary behaviour.

3.1 Helium-flash-driven mixing and carbon ingestion

For stars with metallicity at or below 10^{-5} and masses at or below $2 M_{\odot}$ He-FDM can occur (Fujimoto et al. 1990). He-FDM occurs when a convective zone, driven by helium burning, penetrates into hydrogen-rich regions mixing protons into the carbon-rich parts of the star. This can happen either during the helium flash on the red giant branch or during the TP-AGB phase. It is the latter case that concerns us here. The outer edge of the intershell convective zone (ICZ), generated by helium burning, extends into layers containing hydrogen. Hydrogen is then ingested by the convective zone and is mixed down to a depth where the temperature is much hotter than the hydrogen burning shell. As a result, the hydrogen-burning luminosity increases substantially. This leads to the convective zone splitting into two parts. The upper convective shell is now driven by hydrogen burning, while the lower convective shell is still driven by helium burning. As more hydrogen is mixed into the hydrogen convective shell from above, the hydrogen flash develops further. After the decay of the flash, the region formerly occupied by the hydrogen-driven convective shell is carbon- and nitrogen-enhanced because of the mixing of material from the helium-burning shell. Then the base of the convective envelope penetrates into the layers formerly occupied by the hydrogen burning shell and brings carbon and nitrogen to the surface.

Fig. 3 shows an example of a star undergoing FDM, in

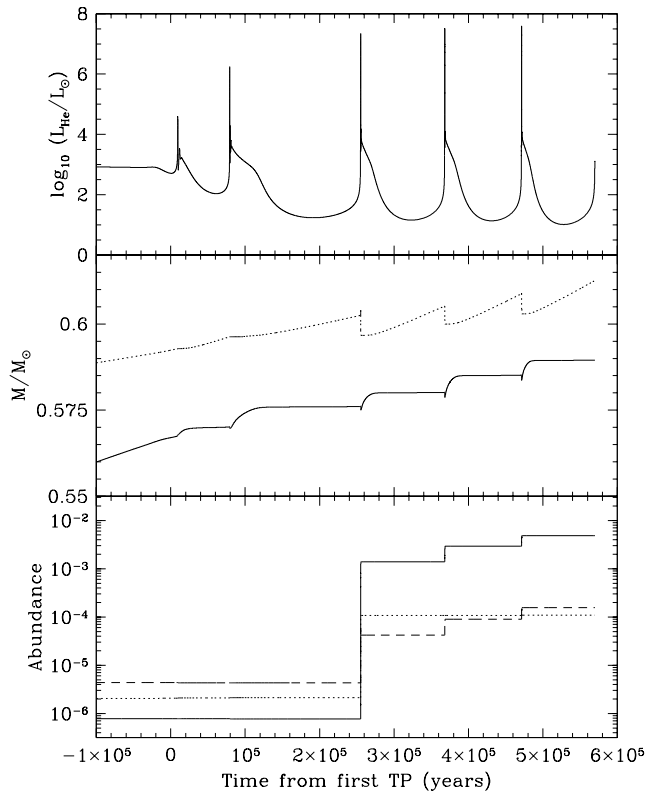


Figure 4. Top panel: helium luminosity as a function of time since the first thermal pulse. Middle panel: H-exhausted core mass (dotted line) and He-exhausted core mass (solid line) as a function of time. Bottom panel: abundance by mass fraction of carbon (solid line), nitrogen (dotted line) and oxygen (dashed line). These plots are for the $1.5 M_{\odot}$ model at $Z = 10^{-5}$. The model undergoes an episode of FDM after about 2.5×10^5 yr since the first thermal pulse, leading to enhancements in the CNO abundances. Thereafter, only carbon and oxygen are enhanced.

this case a $1.5 M_{\odot}$ star of metallicity $Z = 10^{-5}$. At around model number 55000, the convective zone, driven by helium burning, penetrates the hydrogen-burning shell. This causes the hydrogen luminosity to peak. The increased hydrogen luminosity drives a convective zone which connects with the intershell convective zone. Material is then mixed between the hydrogen burning shell and the top of helium burning shells and so there is significant carbon present in the hydrogen-burning shell. Later, around model number 60000, the convective envelope deepens and reaches the region that has been previously mixed. In this way, the products of helium burning are dredged up to the surface during the He-FDM episode. Nitrogen is also dredged up because the CNO cycle converts carbon into nitrogen.

Fig. 4 shows that the surface abundances of CNO elements are enhanced significantly during the He-FDM episode, corresponding to the third pulse of the $1.5 M_{\odot}$, $Z = 10^{-5}$ model. The surface abundance of carbon increases by more than 3 orders of magnitude to the order of 10^{-3} because helium burnt materials are dredged up to the surface. Nitrogen increases from about 2×10^{-6} to 10^{-4} while oxygen increases by one order of magnitude to about 4×10^{-6} .

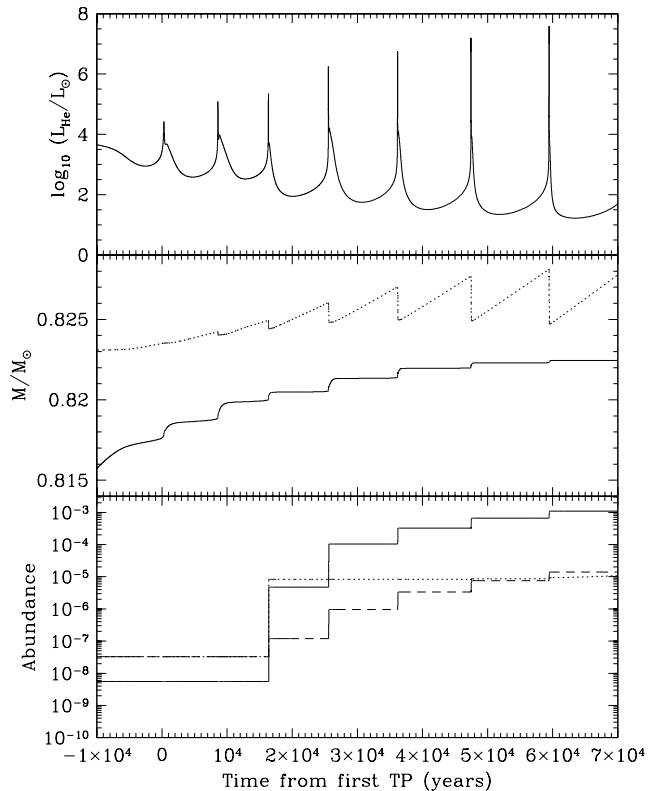


Figure 5. Top panel: helium luminosity as a function of time since the first thermal pulse. Middle panel: H-exhausted core mass (dotted line) and He-exhausted core mass (solid line) as a function of time. Bottom panel: abundance by mass fraction of carbon (solid line), nitrogen (dotted line) and oxygen (dashed line). These plots are for the $3M_{\odot}$ model at $Z = 10^{-7}$. This model suffers the CI mechanism and the first episode of TDUP leads to enhancements of C, N and O.

It is also worth noting that after the He-FDM episode, the surface CNO abundances resemble those of a much higher metallicity star. As a result of higher CNO abundances in the hydrogen burning shell, the helium convective zone cannot any longer reach the hydrogen burning shell in the subsequent pulses and the star behaves similarly to a higher metallicity star. Carbon and oxygen are slowly enhanced during subsequent pulses by third dredge up just as in higher metallicity stars.

We find that FDM episodes only occur for the lowest stellar masses ($2M_{\odot}$ and below). Stars of higher mass do not have violent enough thermal pulses to drive the ICZ up into the H-depleted regions. However they do have pulses that are violent enough to trigger TDUP. Once TDUP has raised the CNO abundance sufficiently, H-burning in the shell proceeds efficiently via the CNO cycle, the H-shell presents an effective energy barrier to the ICZ and prevents any FDM.

At $Z = 10^{-6}$ there is a change in the evolution of the $3M_{\odot}$ and $4M_{\odot}$ star. We find that an extra convective zone, located above the hydrogen burning shell, opens after the peak helium luminosity of the thermal pulse. Unlike the FDM mechanism, this convective zone is not a breakaway region from the intershell convection zone, but is distinctly

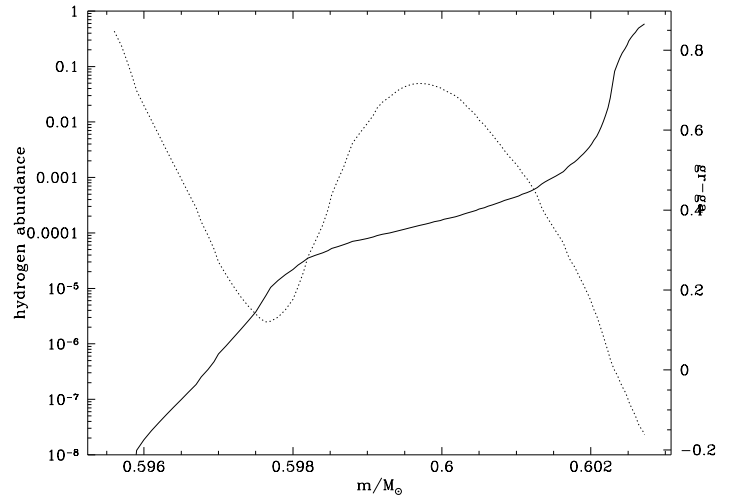


Figure 6. FDM hydrogen abundances (solid line) and $\nabla_r - \nabla_{ad}$ (dotted line) of our $1.5M_{\odot}$, $Z = 10^{-5}$ model during flash driven mixing. A region is convective if $\nabla_r - \nabla_{ad} > 0$. The intershell convective zone reaches the H-burning shell, where the abundance of hydrogen is around 0.1. As a result, plenty of protons are mixed down to regions with higher temperature and carbon abundances.

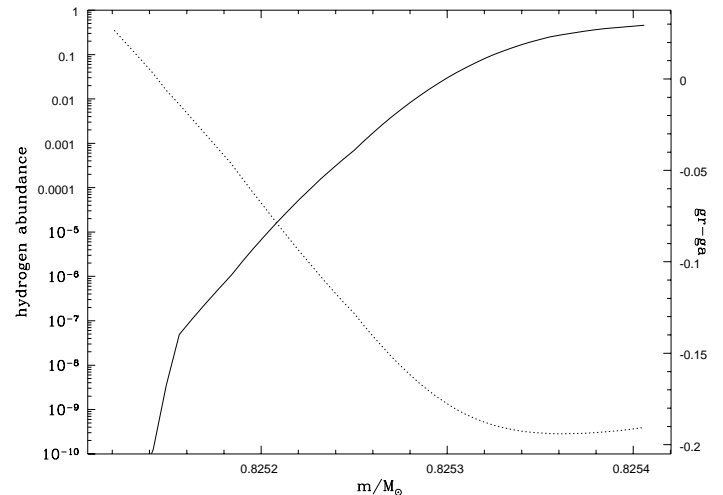


Figure 7. CI hydrogen abundances (solid line) and $\nabla_r - \nabla_{ad}$ (dotted line) of our $3M_{\odot}$, $Z = 10^{-7}$ model during carbon ingestion. A region is convective if $\nabla_r - \nabla_{ad} > 0$. The intershell convective zone reaches the tail H-burning shell, where the abundances of hydrogen is around 10^{-7} . Compared to FDM, far fewer protons are mixed, though still enough to drive a convective zone by the increased hydrogen burning luminosity.

separated from it. This mixing episode is referred to as a CI by Chieffi et al. (2001) and Siess et al. (2002). As described by these authors, carbon from the intershell is injected into the H-burning shell by this convective zone. This mechanism also occurs at $3 - 6M_{\odot}$, $Z = 10^{-7}$ and $3 - 4M_{\odot}$, $Z = 10^{-8}$ models. An example of a star that undergoes this process is shown in Fig. 5

We note that there is a distinction between the nature of flash-driven mixing (FDM) and carbon injection (CI). The FDM phenomenon involves protons being mixed down into

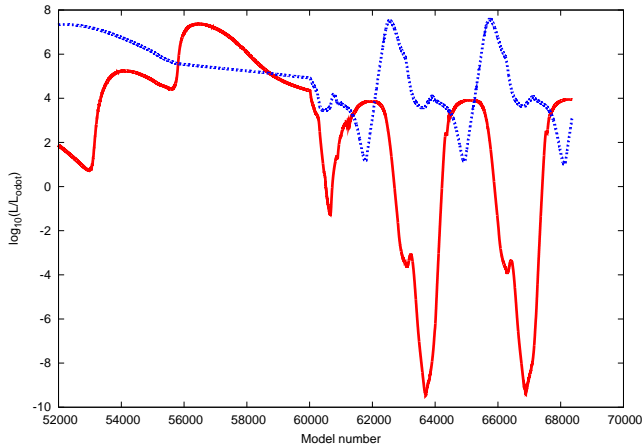


Figure 9. Hydrogen luminosity (solid line) and helium luminosity (dotted line) evolution of a $1.5M_{\odot}$ model at $Z = 10^{-5}$. The hydrogen luminosity reaches $10^7 L_{\odot}$ during the FDM at around model number 56,000.

the intershell region and burning at very high temperatures. For the CI phenomenon, mixing occurs when a convective pocket opens up above the H-shell and its lower edge penetrates down into C-rich regions. H-burning takes place at much lower temperatures than FDM. In addition, the FDM involves the ingestion of a small quantity of hydrogen into a carbon-rich region. Conversely, CI involves the injection of a small amount of carbon into an H-rich region while the amount of hydrogen mixed is minimal.

In both cases, a convective zone opens up at the top of the hydrogen burning shell, so when the third dredge-up deepens, both mechanisms lead to substantial enrichments of nitrogen, though both have only a single episode of N-enhancement. Once TDUP has occurred the CNO abundance is high enough that the star evolves like a higher metallicity star. Are these two distinct phenomenon? Both are triggered by the ingestion of protons in to the intershell convection zone (see e.g. Siess et al. 2002, for the case of the CI). Perhaps it is just the quantity that is ingested that determines which episode a given star experiences.

We suggest that proton ingestion and He-FDM may have the same origin, namely the mixing of protons into a carbon rich region but the amount of hydrogen and carbon mixed determines whether the two convective zones connect each other and hence whether CI or He-FDM occurs. Figs 6 and 7 show how the convective zone reaches the hydrogen burning shell in the FDM and CI events respectively. The convective region penetrates the burning shell and reaches regions where the hydrogen abundance is as high as 0.1 during a FDM event, while it only reaches the tail of the burning shell, where the hydrogen abundance is about 10^{-7} , in the CI episode. In both cases, the mixing of protons and carbon causes an increase of hydrogen luminosity. In the case of FDM the burning is much more vigorous so a larger convective zone is driven and the mixing between the hydrogen burning and helium burning layer is more efficient.

Figs 3 and 8 show the internal structure around hydrogen burning shell of two stars during FDM and CI respectively. In the case of FDM, the vigorous hydrogen burning immediately drives a convective zone that connects with the

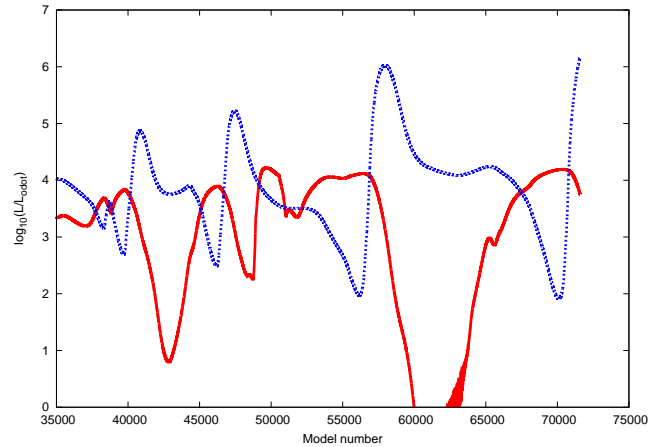


Figure 10. Hydrogen luminosity (solid line) and helium luminosity (dotted line) evolution of a $3M_{\odot}$ model at $Z = 10^{-7}$. The hydrogen luminosity rises to a second peak of $10^4 L_{\odot}$ (around model number 48,000) in the second pulse and this does not occur in the other pulses. It corresponds to the CI.

intershell convective zone. In the case of CI, the burning-driven convection zone appears later in time and is never connected with intershell convective zone while it is extant. FDM mixes material from the H-burning shell with material from He-burning shell in a single large convection zone. For CI the mixing is a two-step process. As a result, when third dredge up occurs later, more carbon is dredged up to the surface in a FDM episode than a CI episode.

In Figs 9 and 10, we see there is a increase of hydrogen luminosity after a thermal pulse which correspond to when FDM and CI occurs. This is unusual. The hydrogen luminosity usually decreases monotonically after a thermal pulse as in the later pulses. We can see that the increase of hydrogen luminosity occurs after the intershell convective zone reaches the hydrogen burning shell by comparing the model numbers with Figs 3 and 8. The increase of hydrogen luminosity starts at model number 55580 for the FDM and at model 48672 for the CI. Compared with Figs 3 and 8, we can see that the increases of luminosity just precedes the opening of the second convection zone around the hydrogen shell. This is because the convective zone around hydrogen burning shell is driven by the increased hydrogen luminosity following the mixing by intershell convective zone. The increase of hydrogen luminosity is much higher in FDM than CI. The hydrogen luminosity jumps to $10^7 L_{\odot}$ in the case of FDM and $10^5 L_{\odot}$ in CI. The peak of the hydrogen luminosity is unsurprisingly correlated with the number of protons mixed into the burning region. The FDM case shows a much stronger peak because the convective shell penetrates through the hydrogen burning shell and causes more mixing than following the CI episode.

In terms of the effect on surface abundances, the distinction between FDM and CI is not so clear cut in some cases. In fact, a model with CI but near the FDM-CI boundary can dredge up almost as much carbon as a model with FDM. On the other hand, models with CI, but near the boundary with normal AGB evolution, dredge no more than in normal third dredge-up. In some situations, more nitrogen than carbon is dredged up after CI. This is because the star also undergoes

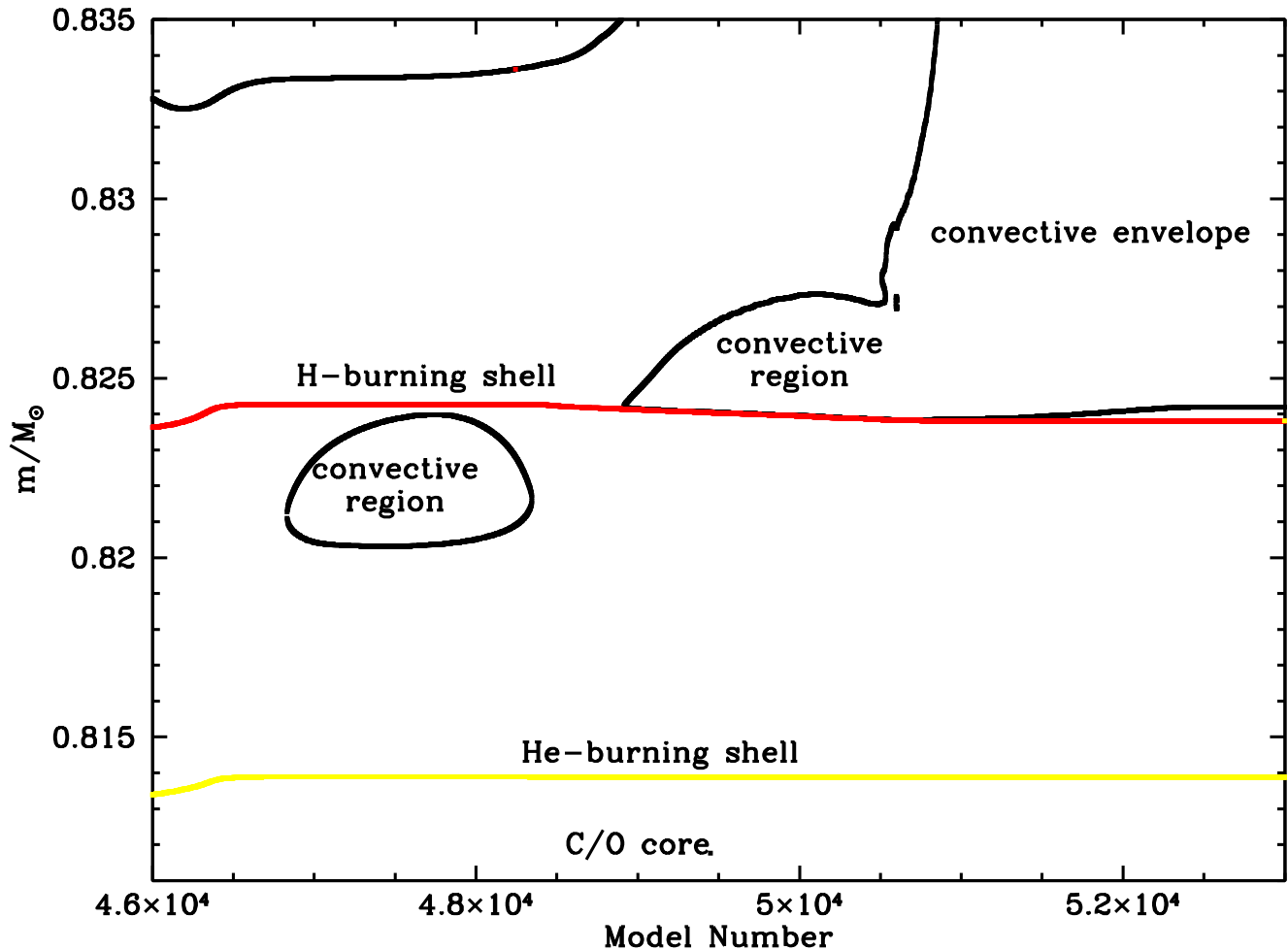


Figure 8. Evolution of a $3 M_{\odot}$, $Z = 10^{-7}$ model during CI. We can see the intershell convective zone reaches the tail H-burning shell at model number around 47000. Then a convective region driven by hydrogen burning reaches deep enough to previously mixed region by the intershell convective zone around model number 50000. At around model number 50500, the convective envelope deepens and connect with the convective zone driven by hydrogen burning. The third dredge up thus dredged up carbon and nitrogen indirectly

hot bottom burning which convert carbon into nitrogen. In general, the effect of CI is stronger when metallicity is lower. This could be because at lower metallicity, the abundance of carbon at the hydrogen burning shell is lower, so the carbon ingested causes a much larger increase in the hydrogen luminosity, which drives a more extensive convective zone.

3.2 Hot dredge-up

In stars of $4 M_{\odot}$ and above, we find some differences in the dredge-up process. For the more massive stars, we note the occurrence of what has been referred to as hot third dredge-up (HTDUP). This phenomenon was described in detail by Herwig (2004). Here, the temperature at the base of the convective envelope at the point when third dredge-up occurs is so high that carbon is converted to nitrogen, resulting in a simultaneous enhancement of both carbon and nitrogen. HTDUP is an extremely efficient dredge-up, with the envelope reaching almost to the bottom of the intershell (or

perhaps beyond it, if overshooting is included, see Herwig 2004 for further details). The behaviour of an example of a star that undergoes this process is shown in Fig. 11. CI occurs at the first episode of third dredge up in this model and the CNO abundances are drastically increased. Then hot third dredge up sets in after two more pulses, leading to simultaneous increase in carbon and nitrogen. Hot bottom burning converts carbon into nitrogen and nitrogen becomes more abundant than carbon by more than one order of magnitude.

3.3 A metallicity threshold for dredge-up?

As we move to the lowest metallicity, we find that TDUP ceases altogether for some models. The $5 M_{\odot}$ model, with $Z = 10^{-8}$ has very weak thermal pulses and these are not strong enough to bring the convective envelope into contact with the C-rich intershell. On the other hand, the $6 M_{\odot}$ model, with $Z = 10^{-8}$ does have a third dredge up. The

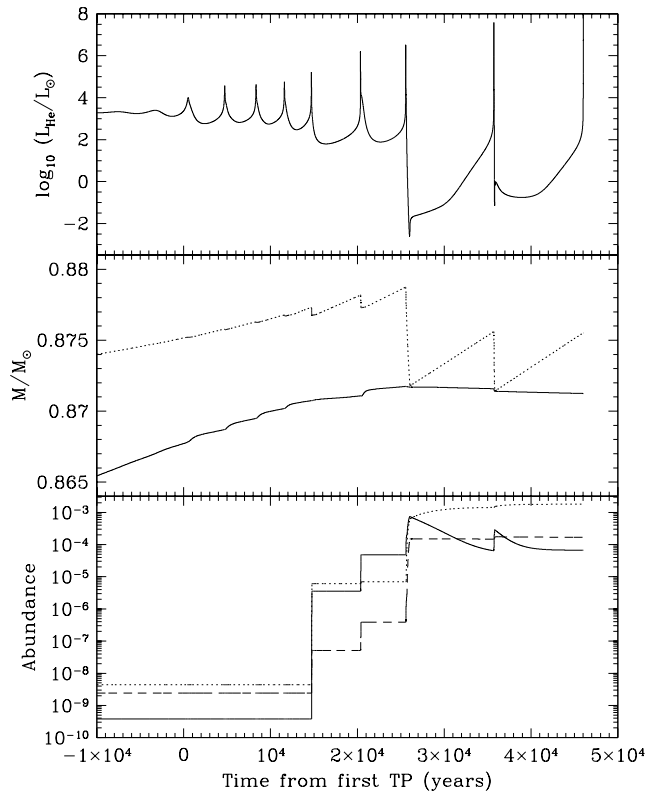


Figure 11. Top panel: helium luminosity as a function of time since the first thermal pulse. Middle panel: H-exhausted core mass (dotted line) and He-exhausted core mass (solid line) as a function of time. Bottom panel: abundance by mass fraction of carbon (solid line), nitrogen (dotted line) and oxygen (dashed line). These plots are for our $4M_{\odot}$ model at $Z = 10^{-8}$. The first episode of TDUP, while extremely shallow, dramatically enhances the CNO abundances. HTDUP sets in after about 25,000 yr, leading to a simultaneous increase in carbon and nitrogen before HBB takes over in the interpulse.

CNO content of the $6M_{\odot}$ in the hydrogen burning shell is higher than the $5M_{\odot}$ because of deeper second dredge up. This seems to confirm the strength of the pulses are dependent on the CNO abundances in the hydrogen burning shell, as suggested by Lau et al. (2008).

The issue of the efficiency of third dredge-up is a perennial problem for modellers of AGB stars. Different stellar evolution codes give very different predictions for the efficiency of TDUP. Some of the reason for this uncertainty is due to the mathematical treatment of the boundaries between radiative and convective regions. Whether one includes convective overshooting at the boundary may also affect the depth of dredge-up. For example, Chieffi et al. (2001) find that third dredge up does occur in their zero-metallicity intermediate mass AGB stars. Chieffi et al. (2001) treated the convective boundaries according to the prescription of Herwig et al. (1997), who use a mixing scheme so efficient that the composition discontinuity between the two burning shells is smoothed out. This seems to indicate the efficiency of third dredge-up depends on the treatment of convection and the inclusion of extra-

mixing mechanisms such as convective overshooting. However, Gil-Pons et al. (2007) find that the total amount of mass dredged-up is very small even when overshooting is included. The STARS code employs an arithmetic mean when computing the mixing coefficient at the convective boundaries. While this means we are mixing in material that lies outside the formal Schwarzschild boundary, it is a far smaller degree of overshooting than applied by other authors but a degree that leads to a stable composition and convection profile. We discuss the effects of overshooting in more detail in Section 4. We find that the inclusion of convective overshooting in our model is enough to cause third dredge up to occur at $Z = 10^{-8}$.

See Lau et al. (2008) for a more detailed discussion and description of the absence of third dredge-up. We notice that the $5M_{\odot}$, $Z = 10^{-8}$ star does not show third dredge-up. Also thermal pulses are growing weaker and weaker and eventually stop after 560 pulses in $5.5 \times 10^5 yr$. Then the star enters a quiescent burning phase which lasts until carbon ignites degenerately at the centre when the CO core mass is $1.36M_{\odot}$. This agrees with the conclusion that supernovae Type 1.5 are likely to be the fate of these stars because of the faster core growth rate when thermal pulses cease (Lau et al. 2008).

3.4 2nd dredge up

Fig. 2 shows the abundance of the CNO elements at the surface of each star at the beginning of the TP-AGB. We note that second dredge-up can lead to substantial enhancement of the CNO abundance. Of particular note is the $5M_{\odot}$, $Z = 10^{-6}$ model, which has a surface CNO abundance that is about ten times higher than its initial metallicity. This enhancement in metallicity is sufficient to allow the star to experience a relatively normal TP-AGB. More CNO strengthens the entropy barrier and decreases the H-tail from the H-burning shell. Note that at the same metallicity, the $3M_{\odot}$ star experiences a CI phenomenon. Also, for the same mass, as we move to lower metallicity, the behaviour changes suddenly as we drop the initial metallicity by just a factor of ten.

3.5 Zero-metallicity models

For stars at zero metallicity, the behaviour is similar to stars with $Z = 10^{-8}$. In the $2M_{\odot}$ model, there is FDM at the first thermal pulse. For the $3M_{\odot}$ model, the evolution is much more complicated. During the first pulse there is a CI phase but it is rather weak and does not increase the surface metallicity by much. There is then FDM at the second thermal pulse. The $4M_{\odot}$ model encounters CI in the first pulse. The thermal pulses of the $5M_{\odot}$ and $6M_{\odot}$ model are not strong enough to cause any third dredge up and probably end their lives as type 1.5 supernovae (Lau et al. 2008).

3.6 Comparison to models from literature

Campbell & Lattanzio (2008) have published a grid of models for $M/M_{\odot} = 0.85, 1.0, 2.0, 3.0$ and the metallicity $[Fe/H] = -6.5, -5.45, -4.0, -3.0$ and $Z = 0$. Our results for $2M_{\odot}$ models agree well with their models. They

find FDM (referred as “Dual Shell Flash” by them) at metallicity $[\text{Fe}/\text{H}] = -4.0$ or below but not at metallicity $[\text{Fe}/\text{H}] = -3.0$. This agrees with our result that the critical metallicity for FDM to occur is between $Z = 10^{-6}$ to 10^{-5} , corresponding to $[\text{Fe}/\text{H}]$ between -4.3 and -3.3 . For their $3 M_{\odot}$ models FDM does not occur at $[\text{Fe}/\text{H}] = -4.0$ or above but does when $[\text{Fe}/\text{H}] = -5.45$ and below. Our result is somewhat different. We only find the milder CI episode instead of FDM in all our $3 M_{\odot}$ models except when $Z = 0$. CI begins to occur between $Z = 10^{-6}$ and 10^{-5} ($[\text{Fe}/\text{H}] = -4.3 - -3.3$) and this agrees with their metallicity range for FDM at $3 M_{\odot}$. For $1 M_{\odot}$ models we find the critical metallicity for flash driven mixing to be between $Z = 10^{-5}$ and $Z = 3 \times 10^{-5}$ ($[\text{Fe}/\text{H}] = -3.3 - -2.8$). This agrees with the fact that FDM already occurs in their model with metallicity $[\text{Fe}/\text{H}] = -3.0$.

One significant difference between the two sets of models is the issue of hot bottom burning. Hot bottom burning does not occur for any of our models with initial mass $3 M_{\odot}$ or below, while their $2 M_{\odot}$ and $3 M_{\odot}$ models have strong hot bottom burning. Therefore, nitrogen is more abundant in their $2 M_{\odot}$ and $3 M_{\odot}$ models, while carbon is more abundant in our models. Hence, it is easier to form CEMP stars with $[\text{C}/\text{N}] \approx 1$ from our models.

Komiya et al. (2007) give an up-to-date version of the dependence of FDM and the third dredge up on the initial stellar mass and metallicity, formulated by Fujimoto et al. (2000). Our models show a few differences to their picture. Their critical metallicity for FDM to occur is $[\text{Fe}/\text{H}] = -2.5$. This is higher than the critical metallicity found in our grid of models ($[\text{Fe}/\text{H}] = -3.3$ to -2.8). Moreover, in their picture, the critical metallicity for FDM to occur is the same for initial masses between $0.8 M_{\odot}$ to $3.5 M_{\odot}$. This is not the case in our models (Fig. 1) where the critical metallicity for FDM to occur in $2 M_{\odot}$ stars is lower than that of $1 M_{\odot}$ and $1.5 M_{\odot}$ stars. Our mass range for FDM is also smaller than their picture.

Another important difference is the nitrogen surface abundances. Their picture shows that extremely metal-poor stars between $3.5 M_{\odot}$ to $5 M_{\odot}$ could be carbon rich but nitrogen normal. However, most of our $4 - 6 M_{\odot}$ models are nitrogen rich due to hot dredge-up. We agree that there are metal-poor stars that have no third dredge up but the mass range from our models is much smaller than theirs.

4 THE EFFECT OF OVERSHOOTING

The above behaviour raises an interesting question: what is the effect of the inclusion of convective overshooting on the behaviour of the models? To examine this, we have constructed a grid of models with convective overshooting. We use the prescription of Schröder et al. (1997) and their overshooting parameter, $\delta_{\text{ov}} = 0.12$. This overshooting is applied up to the beginning of the TP-AGB in all models made.

Fig. 12 shows the abundance of the CNO elements at the surface of each star at the beginning of the TP-AGB. As with the non-overshooting case, we find that second dredge-up can lead to substantial enhancement of the CNO abundance. The effect is even more substantial with the inclusion of overshooting. This is what we would expect to find. We also note that we get a substantial elevation of the CNO

abundance at lower initial masses. With overshooting our $5 M_{\odot}$, $Z = 10^{-8}$ model is significantly enhanced in CNO elements. The CNO abundances of $4 - 6 M_{\odot}$, $Z = 10^{-7} - 10^{-8}$ models with overshooting prescription is higher than models without overshooting by about one order of magnitude.

Unfortunately we are not able to evolve some models along the whole TP-AGB with convective overshooting, owing to as yet unresolved numerical difficulties during hot dredge-up for some stars. These models fail to converge at the onset of hot dredge-up if overshooting is applied. We therefore evolve without the overshooting just before the start of hot dredge-up. Fortunately we can evolve some models, such as the $4 M_{\odot}$, $Z = 10^{-5}$, through a significant number of thermal pulses with overshooting and, based on these models, we believe the inclusion of overshooting during the TP-AGB phase does not significantly affect the subsequent evolutionary behaviour.

Models with overshooting have higher core masses when they enter the TP-AGB phase because of the more extended convective cores during core He-burning. Also, the amount of CNO elements dredged up is higher when overshooting is included. As a result, a model with a given mass and metallicity with overshooting behave more like a model with higher mass without overshooting. Comparing the evolutionary behaviour with overshooting and without overshooting, we see that the major effect is to shift the boundary of different regimes of behaviour by mass but not metallicity (Fig. 13).

We do not find any flash driven mixing or carbon ingestion in stars with $Z = 10^{-4}$ as in the case of models without overshooting. At $Z = 10^{-5}$ the overshooting models of $2 M_{\odot}$ show the occurrence of a relatively weak CI, which is absent in the models without overshooting. The overshooting prescription of STARS code mixes regions where $\nabla_r - \nabla_{\text{ad}} > -0.12$. Therefore, regions that were close to instability can become convective. As a result, a small convective region is opened up and carbon is mixed into proton-rich region.

Unlike models without overshooting, models from $Z = 10^{-6}$ to $Z = 10^{-7}$ do not show any signature of FDM. It is possible that the maximum mass for a model with overshooting to have FDM is just below $2 M_{\odot}$ for metallicities between 10^{-6} and 10^{-7} because a strong CI episode is found in the $2 M_{\odot}$ models at these two metallicities. Flash driven mixing does occur in our $2 M_{\odot}$ model with metallicity at 10^{-8} .

There is a general trend that the upper mass limit for CI increases as metallicity decreases. At $Z = 10^{-5}$ only the $2 M_{\odot}$ model shows a weak CI episode. CI occurs in both the $2 M_{\odot}$ and $3 M_{\odot}$ models at $Z = 10^{-6}$ and in the $2 M_{\odot}$, $3 M_{\odot}$ and $4 M_{\odot}$ models at $Z = 10^{-7}$. At $Z = 10^{-8}$, the $3 M_{\odot}$ and $4 M_{\odot}$ models still encounter CI but the $2 M_{\odot}$ model has a flash-driven mixing episode.

It is worth noting that models of $6 - 7 M_{\odot}$ ignite carbon before any thermal pulses and become super-AGB stars. The $5 M_{\odot}$ models at $Z = 10^{-4}$ and $Z = 10^{-5}$ also enter the SAGB phase before any thermal pulses and we do not model the evolution of these stars. This is in agreement with the general effect of overshooting which causes models to behave like higher mass models.

We also find hot dredge-up in most of the $3 - 5 M_{\odot}$ models, compared to the mass range of $4 - 6 M_{\odot}$ in the non-overshooting models. All of the $4 M_{\odot}$ models encounter hot

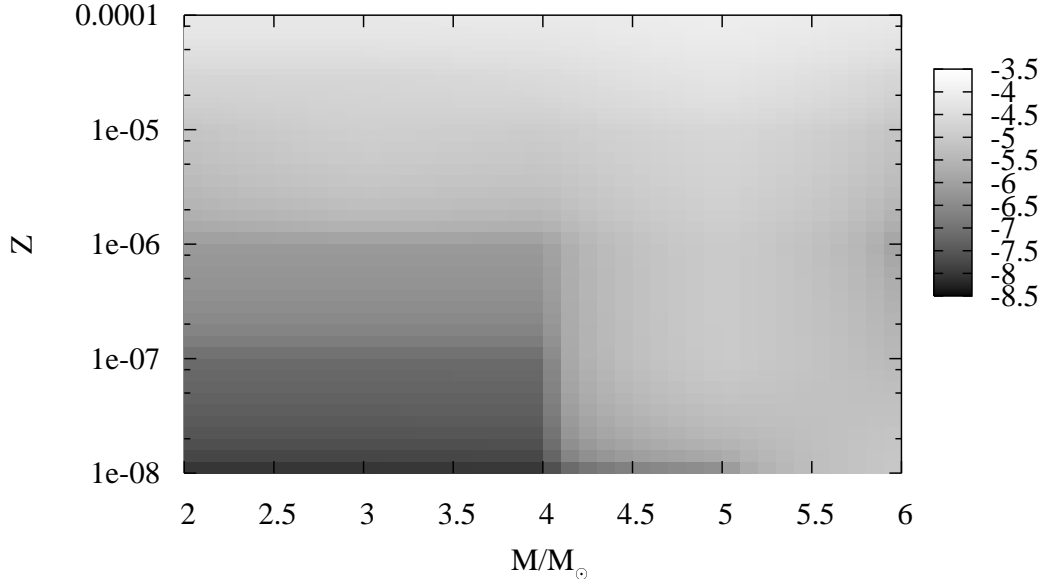


Figure 12. Plot of the logarithm of the abundance of CNO elements by mass at the beginning of the TP-AGB. As is the case of the models without overshooting, the action of second dredge-up substantially raises the abundance in the case of the intermediate mass stars. The additional overshooting makes the effects more pronounced here.

Mass/ M_{\odot}	metallicity	^{12}C	^{14}N	^{16}O	λ
3.0	10^{-4}	2.4×10^{-4}	2.6×10^{-3}	3.0×10^{-4}	3.7
3.0	10^{-6}	2.6×10^{-4}	3.0×10^{-3}	2.8×10^{-4}	3.3
4.0	10^{-4}	7.1×10^{-4}	8.6×10^{-4}	8.1×10^{-5}	5.7
4.0	10^{-5}	3.7×10^{-5}	8.7×10^{-4}	7.4×10^{-5}	7.4
4.0	10^{-6}	3.8×10^{-5}	9.3×10^{-4}	9.8×10^{-5}	5.3
4.0	10^{-7}	3.9×10^{-5}	1.0×10^{-3}	1.0×10^{-4}	6.1
4.0	10^{-8}	1.8×10^{-5}	4.3×10^{-4}	1.4×10^{-5}	4.1
5.0	10^{-6}	1.6×10^{-5}	2.4×10^{-4}	9.0×10^{-6}	4.3
5.0	10^{-7}	1.2×10^{-5}	2.8×10^{-4}	1.0×10^{-5}	4.5
5.0	10^{-8}	2.7×10^{-5}	6.2×10^{-4}	5.8×10^{-5}	2.3

Table 1. Surface abundances by mass fraction after the first hot dredge-up episode and dredge-up efficiency λ of the hot dredge-up episode for models with overshooting.

dredge up. While the two $5M_{\odot}$ models with $Z = 10^{-4}$ and 10^{-5} enter the SAGB branch, the other three $5M_{\odot}$ models with lower metallicities also encounter third dredge up. For the five $3M_{\odot}$ models, we only find hot dredge up in the $Z = 10^{-4}$, $Z = 10^{-6}$ models. Nevertheless, we believe hot dredge up should occur in all $3M_{\odot}$ stars with metallicity ranging from 10^{-4} to 10^{-8} . We did not find the occurrence in some of the $3M_{\odot}$ models because of the earlier breakdown of the evolutionary code owing to unsolved numerical problems.

Hot dredge up occurs at around the 5th pulse at metallicity of 10^{-4} and 10^{-5} . At low metallicity hot dredge up tends to occur in later pulses. In the $5M_{\odot}$, $Z = 10^{-8}$ model it occurs at the 12th pulse. The dredge up efficiency λ ,

defined as the mass dredged up divided by the core mass growth during interpulse phase, is highest for $4M_{\odot}$ models in general (see table 1). The dredge up efficiency seems to remain relatively constant between 10^{-4} and 10^{-7} but is lower at $Z = 10^{-8}$. For $5M_{\odot}$ models the dredge up efficiency is also the same for the $Z = 10^{-6}$ and $Z = 10^{-7}$ models but is lower in $Z = 10^{-8}$. For the two $3M_{\odot}$ models, which show hot dredge up, λ is also similar. In most cases, the code fails to converge at the next pulse after the hot dredge up but in a few, such as the $4M_{\odot}$, $Z = 10^{-6}$ model, we manage to evolve for two pulses with hot dredge up. The dredge up efficiency is much lower in the 2nd pulse, 1.5 compared to 5.3 in the previous pulse.

Also of interest is that the surface abundances after hot

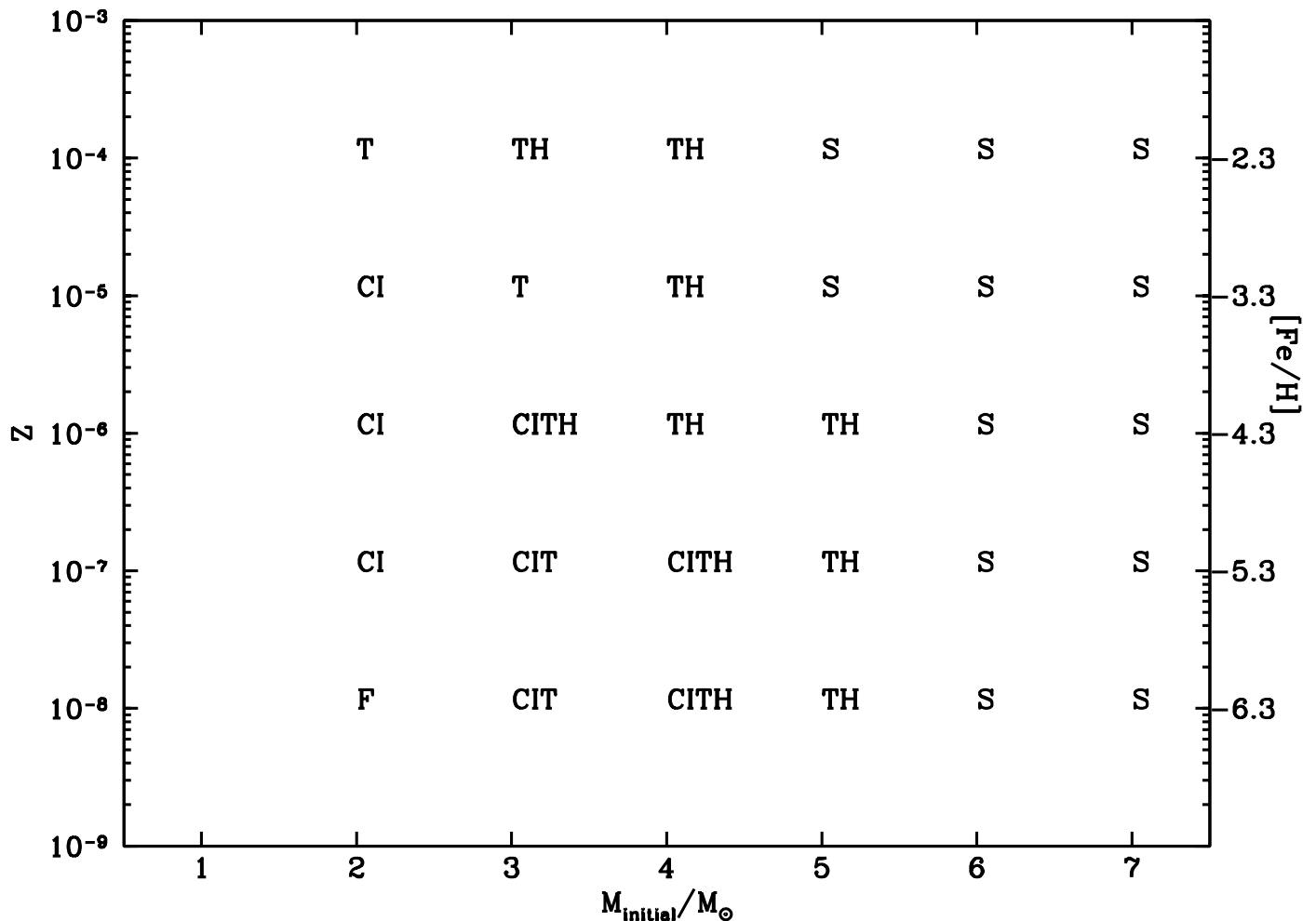


Figure 13. The AGB behaviour of the models as a function of mass and metallicity with overshooting. The symbols are T – third dredge-up, H – hot third dredge-up, F – FDM, CI – CI, X – no TDUP and S – CI before the AGB (presumably leading to an S-AGB star).

dredge do not depend much on metallicity. For $4 M_{\odot}$ models, the surface abundances of carbon are almost constant at 3.8×10^{-5} for $Z = 10^{-5}, 10^{-6}, 10^{-7}$ models (see Table 1). For nitrogen and oxygen, the surface abundances also hardly vary. At $Z = 10^{-4}$ model there is more carbon enhancement than for the $4 M_{\odot}$ models at lower metallicities while the nitrogen and oxygen surface abundances are roughly the same for models with different metallicities. At $Z = 10^{-8}$ the surface abundances of carbon and nitrogen are about half those at higher metallicities while oxygen is down by nearly a factor of ten. The CNO abundances for our $5 M_{\odot}$, $Z = 10^{-6}$ and $Z = 10^{-7}$ stars are almost the same while the $Z = 10^{-8}$ model enriches its surface with more CNO elements by several times. The surface CNO abundances are also very close in the $3 M_{\odot}$, $Z = 10^{-4}$ and $Z = 10^{-6}$ models. This indicates that hot third dredge up wipes out any differences in the initial metallicity of the stars and that subsequently the surface abundances mainly depend on the initial mass.

Amongst our overshooting models we do not find any that do not experience third dredge-up. One possible reason

is that the second dredge up manages to increase the surface metallicity, in particular the CNO elements in the hydrogen shell, above the threshold at which the hydrogen burning shell can be fully sustained by the CNO cycle (Chieffi et al. 2001).

5 CEMP STARS

From our models, we can see that there are a few phenomena that can affect the composition of the material dredged up, namely flash-driven mixing, CI and hot dredge-up. If the material from the envelopes of these stars is accreted on to a binary companion it becomes carbon enhanced. In this section, we compare the surface abundances of our AGB star models results from our code to the observed abundances of different types of CEMP stars to check what types of CEMP stars can be formed by the binary transfer scenario. Objects used in this section are picked from the Stellar Abundances of Galactic Archaeology (SAGA) Internet database

(Suda et al. 2008) and are chosen because their observed abundances fit well the abundances of our models.

Stancliffe & Glebbeek (2008) have discussed the formation of CEMP stars by mass transfer from AGB stars in the mass range $1 M_{\odot}$ to $3.5 M_{\odot}$ with the effect of thermohaline mixing in the secondary. One of the problems they note with the abundances from the AGB models is that they do not predict substantial enhancements of carbon and nitrogen at the same time except in a very narrow mass range. This problem is not solved by the evolution of higher mass AGB models in this work. Although carbon can be brought to the surface in third dredge up in these higher mass models, the presence of hot bottom burning destroys most of it. For example, in the $5 M_{\odot}$, $Z = 10^{-4}$ star without overshooting, $[C/Fe]$ is roughly 1 and $[N/Fe]$ is greater than 3 after hot third-dredge up and hot bottom burning. In the overshooting model, the surface abundances of carbon and nitrogen of the $4 M_{\odot}$ model are roughly equal. In this model, $[C/Fe]$ is equal to 1.6 and $[N/Fe]$ is equal to 2.2 when $[Fe/H]$ is about -2.4 . This could possibly fit the observed abundances of CEMP stars with strong nitrogen enhancement, such as HE 1031-0020. The $3 M_{\odot}$, $Z = 10^{-4}$ model gives a surface abundances of $[C/Fe] = 1.1$ and $[N/Fe] = 2.7$ and may fit star such as HE 0400-2030. However, even with overshooting, the mass range in which we predict substantial enhancement of carbon and nitrogen is indeed narrow.

At a metallicity of $Z = 10^{-4}$, we do not find any flash-driven mixing or carbon ingestion in any of our models. When we move down to the metallicity of $Z = 10^{-5}$, an AGB star could have flash-driven mixing or carbon ingestion or hot dredge-up depending on its mass. More importantly, enhancement of carbon, nitrogen and other elements differs for these three mechanisms. For stars with FDM, the violent nature of the flash causes a very efficient mixing from the helium burning region to the hydrogen burning region. Therefore, when the convective envelope dredges into the region that is previously mixed by the FDM, significant amounts of the CNO elements are dredged to the surface. Carbon can be enhanced by more than 1,000 times (Fig. 3). Nitrogen and oxygen are not enhanced as much and the C/N ratio approaches 100. For example, in the star of $1.5 M_{\odot}$ with $Z = 10^{-5}$ subsequent thermal pulses further increase the carbon and oxygen surface abundance but not nitrogen because the star is not hot enough for hot bottom burning. As a result, the $[C/N]$ ratio can reach 1.5 or higher. Also, the $[C/Fe]$ could be as high as 3. This could explain the formation of HE 1430-0919 which has $[C/Fe] = 2.7$, $[N/Fe] = 1.6$ and $[Fe/H] = -3.01$.

For stars with a CI episode, we find that there is a range of carbon and nitrogen enhancement dependent on the mass of the stars. It is possible for stars with CI to achieve carbon and nitrogen enhancement five times less than the stars with FDM with a similar $[C/N]$ ratio. In some cases, such as the $3 M_{\odot}$, $Z = 10^{-5}$ model with overshooting, the amount of carbon dredged up is lower and $[C/Fe]$ only reaches 2.0 and $[N/Fe]$ only 0.9. This could well explain the formation of stars such as HE 2330-0555 and HE 0017+0055. On the other hand, it is possible that CI could cause the nitrogen abundance to be similar to the carbon abundance as in the case of $3 M_{\odot}$, $Z = 10^{-7}$ without overshooting after the enhancement by CI in the third pulse (see Fig. 5). Whether CI preferentially enhances carbon or nitrogen depends on how

efficiently the star converts carbon into nitrogen and hence depends on the mass and metallicity of the stars. It has to be pointed out that, in the case of $3 M_{\odot}$, $Z = 10^{-7}$ without overshooting, the subsequent third dredge up by later pulses eventually causes the surface carbon abundance to be higher than the surface nitrogen abundance.

For higher-mass AGB stars at this metallicity, the hot dredge up could lead to simultaneous enhancement of carbon and nitrogen. However, while a significant amount of carbon is dredged up, most of it is converted to nitrogen by hot bottom burning, leading to a strong nitrogen enhancement. For example the $4 M_{\odot}$, $Z = 10^{-5}$ stars have surface abundances of $[C/Fe] = 1.3$, $[N/Fe] = 3.1$ and $[Fe/H] = -3.3$. Such nitrogen-rich stars have been searched for but there is an apparent dearth of them (Johnson et al. 2007). As the surface abundances of our models after hot dredge-up does not depend on metallicity, $[N/Fe]$ increases with decreasing metallicity and stars with lower metallicity should have even stronger nitrogen enhancements if metal-poor AGB stars with hot dredge-up do exist.

As we go down in metallicity to about 10^{-7} , the second dredge up of high-mass AGB stars can reach deep enough to penetrate into regions where helium has been burned. Even though third dredge-up is weak or non-existing in such stars, carbon is already enhanced before entering the TP-AGB phase. For example, in the $5 M_{\odot}$, $Z = 10^{-8}$ model with overshooting, just after second dredge-up, carbon is enhanced by a factor of 10^3 while the C/N ratio is around 10. This could potentially be an important way of forming CEMP stars with extremely low-metallicity, such as HE 0107-5240 (Lau et al. 2007). At the moment, we only observe two stars with an iron abundance of less than $[Fe/H] < -5$ (corresponding to $Z = 10^{-7}$ if all the abundances were solar-scaled and the enhancement happened after these stars formed), HE 0107-5240 with $[Fe/H] = -5.3$ (Christlieb et al. 2002) and HE 1317-2326 with $[Fe/H] = -5.45$ (Frebel et al. 2005). However, this scenario cannot explain HE 1317-2326, because of the similar observed enhancement of carbon and nitrogen. In fact, none of our models at such a low metallicity manage to produce a surface abundance with that C/N pattern.

At such low metallicity, the carbon enhancement by high-mass AGB stars through second dredge up can be as significant as that of low-mass stars which go through FDM or CI. At metallicity of 10^{-5} and 10^{-6} , the low-mass AGB stars have stronger carbon enhancement than high-mass AGB stars because FDM or CI leads to more efficient dredge up of carbon than third dredge-up alone.

In conclusion, it is possible to explain CEMP stars with strong carbon enhancement and weaker nitrogen enhancement. They are most likely to be formed from low-mass AGB stars. At $Z = 10^{-4}$ these stars have third dredge up without hot bottom burning, so carbon is strongly enhanced. With metallicity around $Z = 10^{-5}$, both FDM and CI lead to significant carbon enhancement. It is harder to explain stars that have significant enhancement of both carbon and nitrogen. While a narrow mass range of stars at $Z = 10^{-4}$ may be able to enrich carbon and nitrogen significantly through hot dredge-up, most models with hot dredge-up destroy too much carbon and enrich with too much nitrogen to fit the current observations. At a metallicity of 10^{-5} or below, nitrogen-enhanced stars are predicted by our models

but there is currently a dearth of observations of such stars. From our model, it is difficult to explain the existence of CEMP stars that have comparable $[C/Fe]$ and $[N/Fe]$ with $[Fe/H] < -3$. In order to produce stars with both carbon and nitrogen enriched from our model, we need hot bottom burning to be less efficient so less carbon is converted into nitrogen in high-mass AGB stars. If so, it may be possible to match those CEMP stars with both carbon and nitrogen enhanced.

On the other hand, for some stars, there are brief times when both carbon and nitrogen are simultaneously enhanced, such as the $3M_{\odot}$, $Z = 10^{-7}$ without overshooting just after its CI episode but before hot dredge-up. Similarly, an AGB star can be first carbon-rich after the onset of third dredge up and then become nitrogen-rich when hot dredge up kicks in. If mass is transferred from the AGB primary to the companion at suitable time, it is possible for the companion to end up both carbon and nitrogen enhanced. However, this involves a fine tuning of the period of the system and is unlikely to make significant amount of carbon and nitrogen enhanced metal-poor stars.

Finally, we note that the composition of the transferred material may not necessarily be the same as that of an AGB primary which passes through its full TP phase. For example, if the star is in a close binary its life may be truncated if the star fills its Roche lobe or if the presence of a companion enhances its stellar wind. Therefore the binary properties of the system and the evolution of the surface abundances with time are parameters that could affect the observed composition of the secondary. Moreover, the composition of the transferred material is also not necessarily the same as what will be observed on the secondary. Accreted material can become mixed with that of the secondary either through the deepening of the convective envelope when the star undergoes first dredge-up, or via thermohaline mixing immediately after accretion. The consequences of these processes for the surface composition of the secondary are discussed in detail by Stancliffe & Glebbeek (2008) and Stancliffe (2009)

6 THE FEASIBILITY AND PROBLEMS OF DEDUCING THE INITIAL MASS FUNCTION

“What is the initial mass function of metal-poor stars?” is an important question that has no conclusive answer at present. From the abundances of the observed carbon-enhanced metal-poor stars, one could theoretically deduce whether they were formed by binary mass transfer and if so, the initial mass of the primary stars. As a result, it ought to be possible to deduce the initial mass function of metal-poor stars based on the estimated mass of the primary stars.

One important indicator of the primary mass of a particular CEMP star is the nitrogen abundance, in particular the $[C/N]$ ratio, which ranges from -1 to around 1.3 in the observed CEMP stars. As mentioned above, a low-mass AGB star that enhances carbon through FDM or CI has a high $[C/N]$ ratio unless hot dredge up is involved. The C/N ratio is usually 0 to 2 . On the other hand, for the high-mass AGB stars, because carbon is converted into nitrogen, the C/N ratio is much lower. The $[C/N]$ ratio ranges from around -2 to about 0 .

Therefore, based on the observed $[C/N]$ ratio, one might theoretically deduce whether the primary star is a high-mass or low-mass AGB stars. We need more data coming from ongoing surveys such as SDSS SEGUE, from which seven CEMP stars are recently picked and discussed in Aoki et al. (2008). If enough CEMP stars are observed, one might deduce the shape of the IMF of low-metallicity environment by noticing whether low-mass AGB are more numerous or vice versa.

However we currently cannot match all the observed CEMP stars to initial primary masses and so a reliable IMF shape cannot be constructed. In particular, the high-mass AGB stars cannot fit some of the CEMP stars with strong enhancement in carbon and nitrogen and whether we should attribute all those type of stars to high-mass AGB stars would change the result. Though we can draw a general conclusion that a high fraction of CEMP stars with high C/N ratio implies more low-mass AGB primary and vice versa.

On the other hand, our model predicts that both C/Fe and the fraction of CEMP stars increase at lower metallicity. It would be interesting whether such a trend appears when more metal-poor stars are observed, particularly CEMP stars with metallicity $[Fe/H] < -4$. If such a trend is not found observationally or the observed abundances, particularly the C/N ratio, do not fit well with the surface abundances of AGB models, it could be that there is a significant shortcoming to current AGB modelling. Another possibility is that AGB stars did not form and the initial mass function peaked at the massive end below a critical metallicity. If this is the case, other formation channels are needed to explain those CEMP stars.

6.1 The s-process elements

We have not included full nucleosynthesis routines (Stancliffe et al. 2005), so abundances of light elements are not studied. This nucleosynthesis can also indicate whether s-processing has occurred. Without it we do not know if stars with FDM or CI mechanism have any s-process elements. This could be important to deduce the mass of the primary because there are two groups of CEMP stars, one with s-process elements and one without s-process elements.

7 CONCLUSIONS

We have investigated the evolutionary properties of extremely-metal poor AGB stars with $Z = 10^{-4}$ to $Z = 10^{-8}$. We show that for stars with metallicity of $Z = 10^{-4}$, the AGB properties are similar to those of higher metallicity stars, except for the occurrence of hot third dredge up. However, as metallicity decreases, flash-driven mixing or carbon ingestion occurs for low-mass AGB stars. The highest metallicity models for which such phenomena occur is 10^{-5} . We propose CI is a mild version of flash driven mixing.

High-mass AGB stars with masses greater than about $4M_{\odot}$ can undergo hot dredge-up. As a result, the surface C/N ratio of these stars is lower. Surface abundances after hot dredge up depend on mass but not metallicity. The critical metallicity below which third dredge up does not occur is $Z = 10^{-8}$. It is possible for some stars at this metallicity to

completely cease thermally pulsing later in their evolution and end their fate as supernovae type 1.5. (Lau et al. 2008). One model, $5 M_{\odot}$, $Z = 10^{-8}$ without overshooting, is found to have this type of behaviour. However it does not occur with overshooting for stars with $Z = 10^{-8}$. Overshooting also causes the models to behave like a higher mass models without overshooting. In general, the mass boundaries of the different behaviours are shifted by about $1 M_{\odot}$.

We show that the C/N ratio of low-mass AGB stars can be as high as several hundred while the C/N ratio of high-mass AGB stars can be less than one. The variation of carbon and nitrogen enhancement of CEMP stars could then be due to the different initial mass of the primary. However our models here can only explain the CEMP stars with C/N much larger unity and those with C/N around 1/10. They struggle to explain CEMP stars with similar enhancements of carbon and nitrogen. Hot third-dredge up is needed to convert carbon to nitrogen but it is too efficient in our models, destroys too much carbon and produces too much nitrogen to fit the observations.

Theoretically, based on the observed frequency of different C/N ratio of CEMP stars at low metallicity, it is possible to deduce the shape of initial mass function of AGB stars, as stars with large C/N ratio are more likely to accrete mass from low-mass AGB stars.

8 ACKNOWLEDGEMENTS

We thank the referee, Achim Weiss, for his useful comments and suggestions. HBL thanks KIAA for his fellowship and the IoA for support. RJS is funded by the Australian Research Council's Discovery Projects scheme under grant DP0879472. CAT thanks Churchill College for his fellowship.

REFERENCES

- Anders E., Grevesse N., 1989, *Geo.Cosmo.Acta*, 53, 197
Aoki W., Beers T. C., Sivarani T., Marsteller B., Lee Y. S., Honda S., Norris J. E., Ryan S. G., Carollo D., 2008, *ApJ*, 678, 1351
Böhm-Vitense E., 1958, *Zeitschrift für Astrophysik*, 46, 108
Campbell S. W., Lattanzio J. C., 2008, *A&A*, 490, 769
Chieffi A., Domínguez I., Limongi M., Straniero O., 2001, *ApJ*, 554, 1159
Christlieb N., et al. 2002, *Nature*, 419, 904
Cristallo S., Straniero O., Lederer M. T., Aringer B., 2007, *ApJ*, 667, 489
Eggleton P. P., 1971, *MNRAS*, 151, 351
Eldridge J. J., Tout C. A., 2004, *MNRAS*, 348, 201
Frebel A., et al. 2005, *Nature*, 434, 871
Fujimoto M. Y., Iben I. J., Hollowell D., 1990, *ApJ*, 349, 580
Fujimoto M. Y., Ikeda Y., Iben I. J., 2000, *ApJ.Lett.*, 529, L25
Gil-Pons P., Gutiérrez J., García-Berro E., 2007, *A&A*, 464, 667
Gil-Pons P., Suda T., Fujimoto M. Y., García-Berro E., 2005, *A&A*, 433, 1037
Herwig F., 2004, *ApJ*, 605, 425
Herwig F., Bloeker T., Schoenberner D., El Eid M., 1997, *A&A*, 324, L81
Iben I., 1975, *ApJ*, 196, 525
Johnson J. A., Herwig F., Beers T. C., Christlieb N., 2007, *ApJ*, 658, 1203
Komiya Y., Suda T., Minaguchi H., Shigeyama T., Aoki W., Fujimoto M. Y., 2007, *ApJ*, 658, 367
Lau H. H. B., Stancliffe R. J., Tout C. A., 2007, *MNRAS*, 378, 563
Lau H. H. B., Stancliffe R. J., Tout C. A., 2008, *MNRAS*, 385, 301
Lucatello S., Beers T. C., Christlieb N., Barklem P. S., Rossi S., Marsteller B., Sivarani T., Lee Y. S., 2006, *ApJ Lett.*, 652, L37
Lucatello S., Gratton R. G., Beers T. C., Carretta E., 2005, *ApJ*, 625, 833
Lucatello S., Tsangarides S., Beers T. C., Carretta E., Gratton R. G., Ryan S. G., 2005, *ApJ*, 625, 825
Pols O. R., Tout C. A., Eggleton P. P., Han Z., 1995, *MNRAS*, 274, 964
Schröder K.-P., Pols O. R., Eggleton P. P., 1997, *MNRAS*, 285, 696
Schwarzschild M., Härm R., 1965, *ApJ*, 142, 855
Siess L., 2006, *A&A*, 448, 717
Siess L., Livio M., Lattanzio J., 2002, *ApJ*, 570, 329
Stancliffe R. J., 2009, *MNRAS*, pp in press, arXiv:0812.3187
Stancliffe R. J., Glebbeek E., 2008, *MNRAS*, 389, 1828
Stancliffe R. J., Glebbeek E., Izzard R. G., Pols O. R., 2007, *A&A*, 464, L57
Stancliffe R. J., Izzard R. G., Tout C. A., 2005, *MNRAS*, 356, L1
Stancliffe R. J., Jeffery C. S., 2007, *MNRAS*, 375, 1280
Stancliffe R. J., Lugaro M., Ugalde C., Tout C. A., Görres J., Wiescher M., 2005, *MNRAS*, 360, 375
Stancliffe R. J., Tout C. A., Pols O. R., 2004, *MNRAS*, 352, 984
Suda T., Aikawa M., Machida M. N., Fujimoto M. Y., Iben I. J., 2004, *ApJ*, 611, 476
Suda T., Katsuta Y., Yamada S., Suwa T., Ishizuka C., Komiya Y., Sorai K., Aikawa M., Fujimoto M. Y., 2008, *PASJ*, 60, 1159
Yoon S.-C., Langer N., van der Sluys M., 2004, *A&A*, 425, 207